14th Australasian Fluid Mechanics Conference
Adelaide University, Adelaide, Australia
10-14 December 2001

# Environmental Exchange Flows

**G. N. Ivey**

Centre for Water Research

The University of Western Australia, Western Australia, 6009 AUSTRALIA

## Abstract

Exchange flows refers to the transport between fluid reservoirs with differing fluid properties. The issue of importance is the prediction of the rate of exchange and the study of this problem both historically and dynamically can be thought of as a progression from hydraulics to mixing. This progression is reviewed in this work.

## Introduction

Predicting the rate of exchange between two basins or water bodies with differences in density is of great importance in the fields of environmental fluid mechanics. The rate of exchange and the volume of the basins determine the flushing or residence time in the basins, and the flushing is of central importance to issues such as water quality in both freshwater and marine environments. Well known marine examples include the Red Sea [27], the Black Sea [12]), the Mediterranean Sea [30], and Shark Bay in Western Australia [5] which are connected to the ocean by narrow passages. Freshwater inputs, evaporation, and differential heating and cooling can create the density differences. Once dense flows have passed through the contraction, they can travel great distances and influence large areas, as in the case of density-driven abyssal flows in the ocean passing through narrow gaps in the mid-ocean ridges (eg [31]) and providing the deep connection between major ocean basins.

The strength of the exchange flow is dependent on the strength of the density contrast between the basins, the fluid properties and the nature of the topographic constriction between the basins. In particular, the width of the connection, the local water depth and the length are important. For large-scale systems, the rotation of the earth can also be important [31]. Stommel and Farmer [28] were the first to address this problem in regard to an estuarine application. They argued that the level of mixing within the estuary would affect the density of estuarine water, in turn affecting the rate of exchange between the estuary and the exterior ocean. In other words, there can be a coupling between basin dynamics and exchange flow and the dynamics of the flow are dependent on both basin or reservoir properties and the dynamic properties in the constriction. The roles of the geometry of the constriction, the effects of internal mixing and the effects of flow unsteadiness are each examined in the sections below.

## Internal Hydraulics

Internal hydraulic theory provides a useful tool to examine this problem and a model of exchange flow in the case of flow over a sill and flow through a contraction are shown in Figures 1 and 2, respectively. The relatively narrow constriction connects two infinite reservoirs of fluid with different densities, and the density difference drives a bi-directional exchange flow as shown. Internal hydraulic theory provides a useful model for this flow providing there is no internal mixing of either momentum or mass and the individual layers have constant density and velocity, as shown. This approach has been utilised by a number of authors [1,2,7,20,33] to predict the layer thicknesses and velocities under the assumption of a steady state balance between inertia and buoyancy.

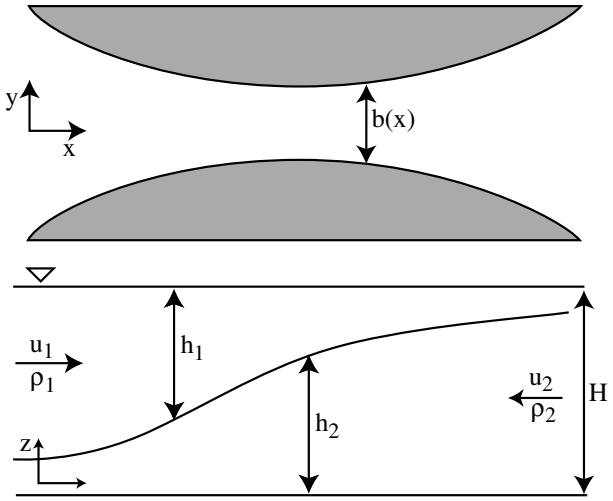


Figure 1. Schematic of the exchange flow through a contraction.

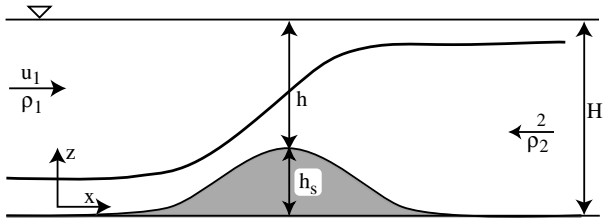


Figure 2 Schematic of the exchange over a sill

If the horizontal variations in channel width and depth are small and the pressure remains hydrostatic, then using conservation of mass in each layer and applying Bernoulli's equation along the surface streamline and at the interface between the two flowing layers, then the rate of change of layer depth can be written as [1]

$$\frac{\partial h_1}{\partial x} = \frac{h_1}{b}\frac{\partial b}{\partial x}\left(\frac{G^2-(1+h_2/h_1)Fr_2^2}{1-G^2}\right) - \frac{\partial h_s}{\partial x}\left(\frac{-Fr_2^2}{1-G^2}\right) \quad (1)$$

$$\frac{\partial h_2}{\partial x} = \frac{h_2}{b}\frac{\partial b}{\partial x}\left(\frac{G^2-(1+rh_1/h_2)Fr_2^2}{1-G^2}\right) - \frac{\partial h_s}{\partial x}\left(\frac{1-Fr_1^2}{1-G^2}\right) \quad (2)$$

where the density ratio is $r = \rho_1/\rho_2$, the internal Froude numbers are $Fr_i^2 = u_i^2/g'h_i$ and the parameter G is the composite Froude number defined as [1]

$$G^2 = Fr_1^2 + Fr_2^2 - (1-r)Fr_1^2 Fr_2^2 \quad (3)$$

Consider first the case of a pure contraction in Figure 1. At the minimum width of the contraction (ie $\partial b/\partial x = 0$) equations (1) and (2) imply either that both layers are flat ($\partial h_i/\partial x = 0$) or from the denominator terms

$$G^2 = 1 \qquad (4)$$

Similarly for the case of a pure sill in Figure 2, at the crest of the sill (ie $\partial h_s/\partial x = 0$) equations (1) and (2) imply either that both layers are flat ($\partial h_i/\partial x = 0$) or again $G^2 = 1$.

At any point in the flow where (4) holds, the flow is said to be controlled as the relationship between the flow variables is constrained, and in these cases it represents a topographic control point [20]. At any other point in the domain where the terms in the numerator of (1) and (2) are zero and again $G^2 = 1$, the point is termed a virtual control [20,33]. If the topographic and virtual control points coalesce, then the flow rates are maximal.

Dalziel [7] showed

$$G^2 = 1 + \frac{C_1 C_2}{h_1 h_2} \qquad (5)$$

where $C_1$ and $C_2$ are the phase speeds of the long internal waves (non-dimensionalised by $1/2(g'H)^{1/2}$). Clearly at control points where $G^2 = 1$, either $C_1$ or $C_2$ must be zero, implying that information can only propagate in one direction only. For supercritical flows where $G^2 > 1, C_1$ and $C_2$ must both be non-zero and of the same sign.

These arguments illustrate the power of the hydraulic approach and the importance of locating control points. For example, for the case of a contraction shown in Figure 1, Armi and Farmer [2] introduced the flow rate ratio $q_r = Q_1/Q_2$ and in the case of steady flow between two infinite reservoirs with no other driving forces, such as tide of wind, then $q_r = 1$. In this case, at the narrowest point of a contraction where $b = B$ the two layers are of equal thickness (ie $h_1 = h_2$) and the volume flux Q and mass flux M in each layer is simply [2,16].

$$Q_i = \left(1/4\right) g'^{1/2} B H^{3/2}, \quad M = \left(1/4\right) \Delta\rho B g'^{1/2} H^{3/2} \qquad (6)$$

In field applications, if a control point is therefore known to exist in the domain, then exchange rates can be directly determined from (6) given the depth and width scales and the density contrast between layers.

In addition to local constraints in the connecting channel, the flow can also be influenced by properties in the reservoir or basins supplying fluid. Finnigan and Ivey [9,10] considered the case shown in Figure 3 with flow over a sill and an enclosed basin on one side. This is a good model for flows in such geophysical examples as the Red Sea, the Mediterranean and Shark Bay. Explicitly addressing the question of how the driving density contrast $\Delta\rho$ is established, they considered the case where the semi-enclosed basin has a net surface buoyancy flux $B_0$ due to net cooling and/or evaporation.

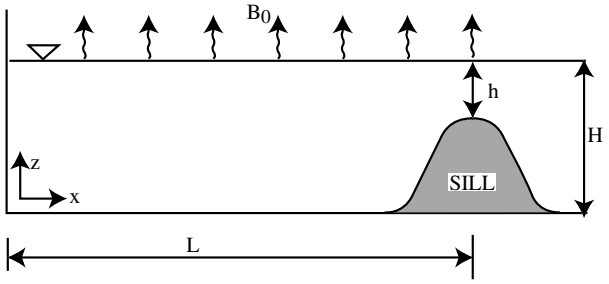


Figure 3. Schematic of convectively driven exchange in a sill-enclosed basin.

At the crest of the sill the flow rates are the same in both layers and a single control point exists in the flow. Using the fact the density ratio $r \approx 1$ in most practical applications, (4) can be re-arranged [9,10] to yield

$$Q = B\left[ g'\left( \frac{1}{h_1^3} + \frac{1}{\left(h - h_1\right)^3} \right)^{-1} \right]^{1/2} \qquad (7)$$

If the system is at steady state, then conservation of buoyancy for the whole basin requires that

$$Qg' = B_0 LB \qquad (8)$$

Hence from (7) and (8)

$$Q = B\left[ B_0 L\left( \frac{1}{h_1^3} + \frac{1}{\left(h - h_1\right)^3} \right)^{-1} \right]^{1/3} \qquad (9)$$

Equation (9) expresses the coupling between the local hydrodynamic balance at the sill crest and the global or basin scale forcing, quantified by the surface buoyancy flux $B_0$ and the length L and width B of the semi-enclosed basin. Providing that the depth of the upper layer $h_1$ is known at the crest of the sill, the problem is closed as $g'$ and Q can be determined from (8) and (9), respectively.

Farmer and Armi [2] argued that in the case of a sill $0.625 < h_1 < h$, and the maximum possible flow rate was achieved when $h_1 = 0.625h$, implying from (9) that the maximal possible flow rate is

$$Q_m = 0.35B(B_0 L)^{1/3} h \qquad (10)$$

The force balance in basin has been examined in several studies [10,13,25,29]. Finnigan and Ivey [10] conducted a laboratory experiment and made measurements of the mean and turbulent velocity fields in the basin. The experiments demonstrated that inertia, buoyancy and friction, associated with the turbulent convection from the free surface, each contribute to the basin scale force balance. The density of the lower layer at the sill reflects the cumulative effect of the mixing processes in the basin. As the surface buoyancy flux $B_0$ increases in intensity, entrainment and recirculation between the upper and lower flowing layers in the basin

increases, and accordingly there is a decrease below the maximal limit predicted in (10). In longer basins (L/H>>10), entrainment is less important. In all cases the flow rates appear to be less than maximal rates yet always characterised by a coupling between basin mixing processes and hydraulic control at the sill.

### Internal Mixing

The arguments above rely on the effect of turbulent mixing of both momentum and mass to be confined to the basin. Crucially, in the constriction region itself these affects can be neglected and theories based on internal hydraulics such as the ones leading to (1) and (2) may apply. But what if there is mixing in the contraction itself? In nature the sources of turbulence responsible for this can include (eg [15]): cooling or evaporation from the free surface leading to a de-stabilising buoyancy flux, wind stress on the free surface, shear stress on the bottom and the internal shear at the density interface. All these mechanisms can provide sources of turbulent kinetic energy which will attempt to overcome the stabilising effects of the potential energy in the water column induced by the horizontal flux of buoyancy through the contraction from the end reservoirs. When there is significant vertical transport of mass and momentum, the basic premises of the hydraulic theories above are no longer valid, and yet field examples of this limit abound (eg Figure 4).

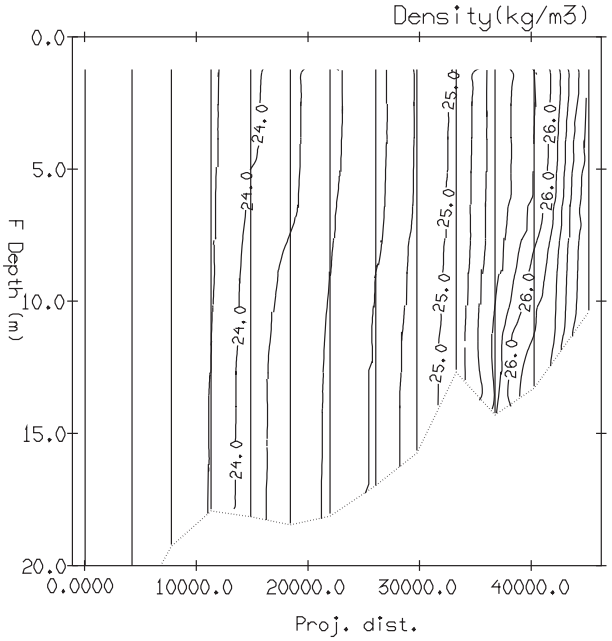


Figure 4. Field data from Shark Bay, Western Australia [23].

The problem of specifying horizontal buoyancy flux when there is significant vertical mixing has been examined in two contexts: estuarine circulation [24] and in the context of heat transfer applications (eg [4]). Under the assumption that the aspect ratio $A = H/L$ is small, Cormack, Leal and Imberger [6] were the first to derive a formal asymptotic solution to the problem defined in Figure 5. The steady state force balance is between buoyancy and turbulent viscous terms, the flow is hydrostatic in the vertical and at leading order reduces to

$$g\frac{\partial \rho}{\partial x} = \rho_0 K_v \frac{\partial^3 u}{\partial z^3} \qquad (11)$$

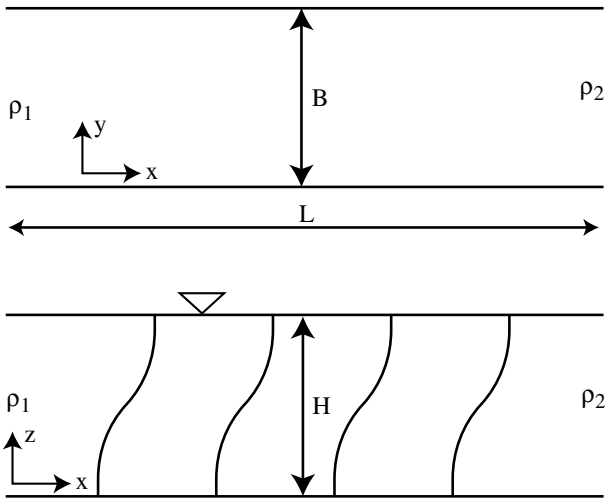


Figure 5. Schematic of density field in viscous-diffusive limit.

At this leading order the density gradient is linear in the horizontal and the volume and mass fluxes can be written as [16]

$$Q = \frac{5}{384} Gr_T A B K_v \qquad (12)$$

$$M = K_\rho A B \Delta\rho + \alpha Gr_T^2 A^3 B K_v \Delta\rho \qquad (13)$$

where $K_\rho$ and $K_v$ are the eddy diffusivities for the stratifying species and momentum, respectively, and the Grashof number $Gr_T = g'H^3/K_v^2$. The mass flux in (13) demonstrates that the horizontal flux is due to both a diffusive component and a convective component as confirmed by laboratory experiments by Imberger [18].

Note that the predictions in (12) and (13) can be non-dimensionalised by their hydraulic limit counterparts in (6). For example the non-dimensional flow rate in the viscous limit

$$q_v = \frac{5\left(Gr_T A^2\right)^{1/2}}{96} \qquad (14)$$

The results in (6) and (12) represent the two limiting conditions, one the hydraulic limit, and the other the diffusive limit. As (14) demonstrates, the naturally occurring parameter that defines the transition between these limits is $Gr_T A^2$.

Between these two theoretical limits, there will be a whole range of possibilities and these were explored in a numerical simulation by Hogg *et al.* [16] using the code developed by Winters *et al.* [32]. The philosophy in the numerical modelling was to use the turbulent diffusivity as an independent free parameter – generated by an unspecified source - to determine it's influence on the exchange rate and in all simulations. It was assumed $K_\rho = K_v$. The results are shown in Figure 6. As the figure demonstrates, the hydraulic limit represents the maximal flow rate and as the intensity of vertical mixing increases (equal to decreasing $Gr_T$) the effectiveness of the horizontal flow decreases. This effect was demonstrated in laboratory experiment [21,22] with air bubbles passed through

the (base of a tank) to simulate the influence of turbulence in the environment on horizontal exchange flows.

The predictions from Hogg *et al.* [16] can be summarised (15).

$$\begin{aligned} &Gr_T A^2 < 40 && m = \frac{4A^2}{\left(Gr_T A^2\right)^{1/2} Pr_T} + \frac{31\left(Gr_T A^2\right)^{3/2} Pr_T}{90720} \\ &40 < Gr_T A^2 < 10^6 && m = 1 - 2.3\left(Gr_T A^2\right)^{-1/4} \\ &Gr_T A^2 > 10^6 && m = 1 \end{aligned} \qquad (15)$$

What is of interest is where in this parameter range typical field cases lie and some examples are shown in Figure 6. Not included is the Shark Bay example in Figure 4, which lies around $Gr_T A^2 = 10^{-1}$. Clearly many examples lie in the transitional regime $40 < Gr_T A^2 < 10^6$ where the flux is neither in the hydraulic limit nor the diffusive limit.

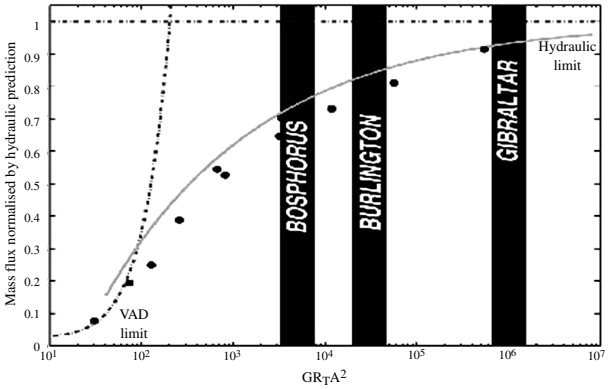


Figure 6. Non-dimensional mass flux vs $GrA^2$ and comparison with field sites.

Not only do turbulent effects retard the buoyancy-driven horizontal exchange as shown in Figure 6, but they can also affect the speed of propagation of waves which control the flow near the hydraulic limit. The concept of control thus must be generalised to continuously stratified fluids where momentum and species are allowed to diffuse. Hogg *et al.* [17] examined the propagation of the gravest vertical mode internal wave within a contracting channel using two approaches. First, waves were mechanically excited at discrete locations within a bi-directional exchange flow. The waves were then tracked in time and space to determine propagation characteristics, under the assumption of linear internal wave dynamics. While useful, it is difficult to extract individual modes, so a second technique based on linear stability theory was employed. In particular, viscous and diffusive terms were retained, leading to a 6th order generalised version of the Taylor-Goldstein equations [19] describing the stability of the flow. This was solved under the assumption that for control we are interested in only the long internal wave (ie small wavenumber) limit.

Both approaches show that as, as in two-layer flows, control may be thought of in terms of information propagation. A single mode, centred on the maximum density gradient, appears to conform to the behaviour for the interfacial mode in two-layer theory. When the phase speed is zero, this location is the point of control. Two other important modes also were found to exist but skewed from the density interface with the maximum in the eigenvector located at the point of maximum vorticity gradient, hence the term vorticity modes [17]. The fundamental difference from hydraulic theory is that there now exists a control region, rather than a point, where over the region control gradually take effect. The overall effect is, however, maintained: end reservoir conditions can change without altering the flow. This has important implications for geophysical flows. In particular, if this allows the determination of whether a channel is super or sub-critical, then flux variations can be determined from changes in external conditions [17].

## Unsteady Flows

In many environmental or geophysical applications unsteadiness is a major issue and it can take two forms. Firstly the time dependency of the boundary conditions or forcing conditions in the basin, and secondly that superimposed on the baroclinic exchange forced by density differences there can be an independent barotropic flow which can be time dependent – for example the tide.

Finnigan *et al.* [11] used a numerical model to investigate the flow field associated with the configuration shown in Figure 3 where the surface forcing condition was allowed to be time dependent, that is $B_0 = B_0(t)$. Various forcing conditions were examined, including both step changes and sinusoidal forcing – reflecting the seasonal variation of forcing that occurs in such systems as the Red Sea, for example. Using an energetics analysis, Finnigan *et al.* [11] developed a general description of the flow response at the sill. In particular, the system can be characterised by a response timescale defined as

$$T_r = 0.3L^{2/3}\Delta B_0^{-1/3}\left(H/h\right) \qquad (16)$$

where $\Delta B_0$ is the magnitude of the buoyancy flux variation. When the forcing frequency $\omega$ is low (ie $\omega << (1/T_r)$), the system is well described by steady state theories and the response at the sill is in phase with the forcing. As the forcing frequency increases, the magnitude of the response decreases at the sill and there is an increasing phase lag. At high frequencies (ie $\omega >> (1/T_r)$), the oscillation of the forcing is completely damped within the system and the flows at the sill is steady at the mean value of the forcing. In terms of application to the Red Sea, for example, this predicts that the flow over the sill always lags behind the seasonal forcing by about 2 months, and flows at the sill never reach more than 90% of the values predicted by steady state theories [11].

A second form of unsteadiness that can be important is when there is a barotropic flow due to a tide superimposed on the baroclinic flow. When a barotropic flow is superimposed on the exchange, the flow rate ratio $q_r \neq 1$ and the position of the virtual control points in a contraction flow is no longer coincident with the topographic control point. More fundamentally, if the barotropic flow is time dependent, the exchange process can be fundamentally altered. This effect has been examined in laboratory experiments by (eg [14]) and recently by Phu [26]. The configuration used by Phu [26] is shown in the schematic in Figure 7. The rocking of the tank is a convenient way to simulate the tidal action. At the start of the experiment, fluid of different densities are placed in each

reservoir and separated by the gate. The experiment is initiated by simultaneously withdrawing the gate and initiating the rocking of the tank.

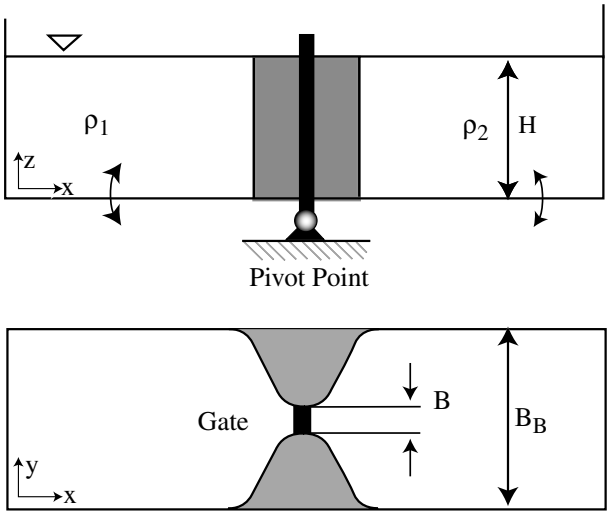


Figure 7. Schematic of unsteady exchange experiment.

The mechanism of exchange is shown in Figure 8. For the basin shown, on the flood phase (Figure 8a) there is a strong jet-like flow entering the basin, while on the ebb flow (Figure 8b) there is a radial draining towards the narrow contraction. The same fluid mass is not transferred in and out of the basin on each half cycle, the difference being a net mass transfer between basins. This configuration enables the estimation of flux, not by direct measurement, but by rather observing the change in reservoir conditions. By opening the dividing barrier at time t=0, and then closing the barrier at time t later after a number of cycles, the fluid in each now closed reservoir is then homogenised and the mean density determined by measurement using a digital densitometer. Since the volume of each reservoir is known, the mass flux can thus be inferred by measuring the increase in mean density in one reservoir and the corresponding decrease in density of the opposing reservoir over the time interval.

The barotropic component has amplitude a and period T. The tidal flux will be given by

$$Q_T = \frac{a}{T} L B_B. \qquad (17)$$

Non-dimensionalising the baroclinic flux in (6) above by (17) yields a tidal exchange parameter defined as

$$E_T = \frac{g'^{1/2} H^{3/2} B_B T}{aLB} \qquad (18)$$

where we have ignored the constant. Measured exchanged flows non-dimensionalised by either (6) or (17) are shown in Figure 9 as a function of this non-dimensional parameter.

As can be seen there are two limiting conditions. For $E_t > 5$, the baroclinic flux dominates and the predicted flow rate from (6) is valid. For $E_t < 0.5$ the tidal forcing dominates and the exchange flux is $Q_T = 0.4\,(a/T)LB$. For the intermediate range where $0.5 < E_t < 5$, both the baroclinic and the unsteady tidal components contribute to the total flux.

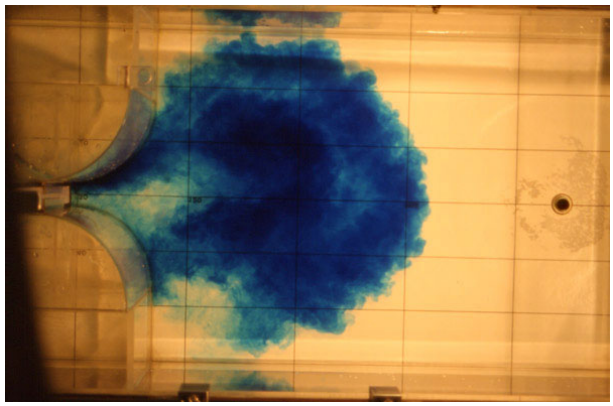

Figure 8(a). Plan view of exchange flow on flood tide.

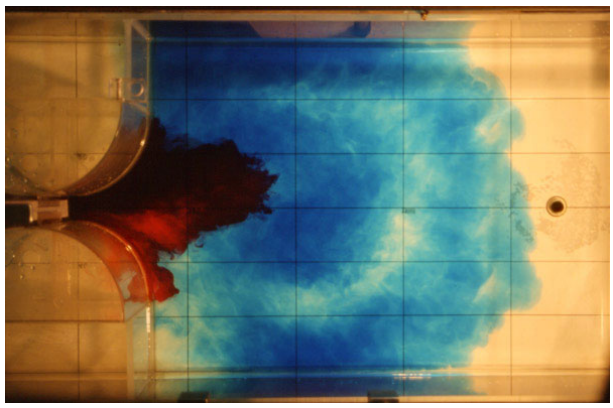

Figure 8(b). Plan view of exchange flow on ebb tide.

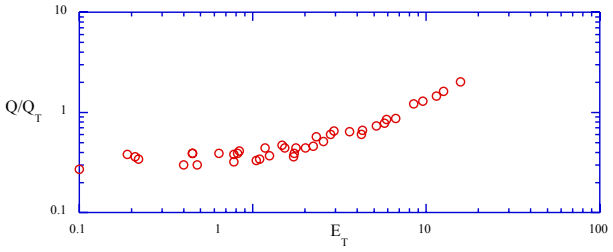


Figure 9(a). Flow rate as a function of tidal exchange parameter (18).

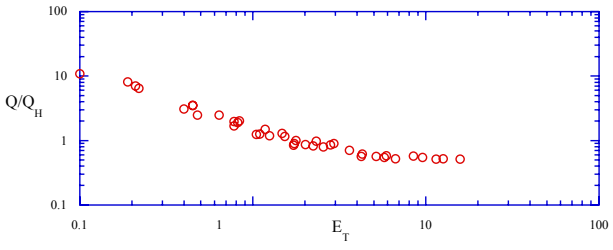


Figure 9(b). Flow rate as a function of tidal exchange parameter from [26].

## Conclusions

As can be seen, the combination of theory and experiment, drawing on contributions from diverse areas of fluid mechanics, have yielded considerable insight into the nature of environmental exchange flows. Recent work has allowed us to

go beyond the predictive capabilities of hydraulic theory by including the effects of turbulence and mixing, not only within the passage where exchange is occurring, but also in the reservoirs which maintain the supply fluid of differing densities that are driving the motion. In the hydraulic limit, flows can be predicted provided it can be demonstrated that control points exist in the flow, usually either at the narrowest points of a contraction or at the crest of sills. In the strong mixing case the concept of hydraulic control is no longer relevant, and rates of exchange are then determined by the magnitude of the parameter $Gr_T A^2$. This, in turn requires an estimate of the effective vertical diffusivity and specifying this quantity in a density stratified fluid is a subject of active research in itself (eg [3]). Finally, the effects of rotation have only been explored in the hydraulic limit (eg [31]) and these large scale flow problems remain a challenge for the future.

## References

[1] Armi, L., The hydraulics of two-layer flows with different densities. *J. Fluid Mech.,* **163**, 1986, 27-58.

[2] Armi, L. and Farmer, D.M. Maximal two-layer exchange through a contraction with barotropic net flow. *J. Fluid Mech.,* **164**, 1986, 27-51.

[3] Barry, M.E., Ivey, G.N., Winters, K.B. & Imberger, J., Measurements of diapycnal diffusivities in stratified fluids. *J. Fluid Mech*., **442**, 2001, 267-291.

[4] Bejan, A., *Convection Heat Transfer*, John Wiley, 1995.

[5] Burling, M.C., Ivey, G.N. and Pattiaratchi, C.B. Convectively driven exchange in a shallow coastal embayment. *Cont. Shelf Res*.,**19**, 1999, 1599-1616.

[6] Cormack, D.E., Leal, L.G. & Imberger, J., Natural convection in a shallow cavity with differentially heated endwalls. Part 1. Asymptotic theory. *J. Fluid Mech*., **65**, 1974, 209-229.

[7] Dalziel, S.B., Two layer hydraulics: a functional approach. *J. Fluid Mech*., **223**, 1991, 135-163

[8] Farmer, D.M. & Armi, L., Maximal two-layer exchange flow over a sill and through a combination of a sill and contraction with barotropic flow. *J. Fluid Mech*., **164**, 1986, 53-76.

[9] Finnigan, T.D. & Ivey, G.N., Submaximal exchange between a convectively forced basin and a large reservoir. *J. Fluid Mech.*, **378**, 1999, 357-378.

[10] Finnigan, T.D. & Ivey, G.N., Convectively driven exchange in a stratified sill-enclosed basin. *J. Fluid Mech.,* **418**, 2000, 313-338.

[11] Finnigan, T.D., Winters, K.B. & G.N. Ivey (2001) Response characteristics of a buoyancy-driven sea. *J. Phys. Oceanogr.*, **31**, 2001, 2721-2736.

[12] Gregg, M.C. , Ozsoy, E. & Latif, M.A., Quasi-steady exchange flows in the Bosphorus. *Geophys. Res. Let*., **26**, 1999, 83-86.

[13] Grimm, Th. & Maxworthy, T., Buoyancy-driven meanflow in a long channel with a hydraulically-constrained exit condition. *J. Fluid Mech.,* **398**, 1999, 155-180.

[14] Helfrich, K., Time-dependent two-layer hydraulics exchange flow. *J. Phys. Oceanogr.*, **25**, 1995, 67-113

[15] Hill, A.E., Buoyancy Effects in Coastal and Shelf Seas, in *The Global and Coastal Ocean, The Sea*, Vol 10, editors K.H. Brink and A.R. Robinson, John Wiley, 1998.

[16] Hogg, A., Ivey, G.N. & Winters, K. B., Hydraulics and mixing in controlled exchange flows. *J. Geophys. Research*, **106**, 2001, 959-971.

[17] Hogg, A.McC., Winters, K.B. & Ivey, G.N., Linear internal waves and the control of stratified exchange flows. *J. Fluid Mech.*, 2001, in press

[18] Imberger, J., Natural convection in a shallow cavity with differentially heated endwalls. Part 3. Experimental Results. *J. Fluid Mech*. **65**, 1974, 247-260.

[19] Kopel, D., On the instability of a thermally stratified fluid under the action of gravity. *J. Meth. Phys*., **5**, 1964, 963-982.

[20] Lawrence, G.A., On the hydraulics of Boussinesq and non-Boussinesq two-layer flows. *J. Fluid Mech.,* **215**, 1990, 457-480.

[21] Linden. P.F. and Simpson, J.E. Gravity-driven flows in a turbulent fluid. *J. Fluid Mech.,* **172**, 1986, 481-497.

[22] Linden. P.F. and Simpson, J.E. Modulated mixing and frontogenesis in shallow seas and estuaries. *Cont. Shelf Res.,* **8**, 1988, 1107-1127.

[23] Nahas, B. Dynamics of Shark Bay. *M.Eng Sc. Thesis, Univ. of W.A*., 2001, in preparation.

[24] Officer, C.B., *Physical Oceanography of Estuaries*. John Wiley and Sons, 1976.

[25] Phillips, O.M., On turbulent convection currents and the circulation of the Red Sea. *Deep Sea Res*., **13**, 1966, 1149-1160.

[26] Phu, A. Tidaly driven excchange flows. *Honours thesis, Dept. Environmental Eng., Univ. of W.A*., 2001.

[27] Pratt. L.J., Johns, W., Murray, S.P. & Katsumata, K., Hydraulic interpretation of direct velocity measurements in the Bab al Mandab. *J. Phys. Oceanogr.*, **29**, 1999, 2769-2784.

[28] Stommel, H. & Farmer, H.G., Control of salinity in an estuary by a transition. *J. Mar. Res.,* **12**, 1953, 13-20.

[29] Tragou, A. and Garrett, C., The shallow thermohaline circulation of the Red Sea. *Deep Sea Res*., **444**, 1997, 1355-1376.

[30] Wesson, J.C. & Gregg, M.C., Mixing at Carmarinal Sill in the Strait of Gibraltar *J. Geophys. Research*, **99**, 1994, 9847-9878.

[31] Whitehead, J.A., Topographic control of oceanic flows in deep passages and straits. *Reviews of Geophys*., **36**, 1998, 423-440.

[32] Winters, K.B. & Seim, H.E., The role of dissipation and mixing in exchange flows through a contracting channel. *J. Fluid Mech.,* **407**, 2000, 265-290

[33] Wood, I.R., A lock exchange flow. *J. Fluid Mech.,* **42**, 1970, 671-687

[34] Zhu, Z. & Lawrence, G.A., Holmboe's instability in exchange flows. *J. Fluid Mech.,* **429**, 2001, 391-409.